Calibration and Spectral Reconstruction for CRISATEL: An Art Painting Multispectral Acquisition System

Alejandro Ribés and Francis Schmitt
Ecole Nationale Supérieure des Télécommunications, Paris, FRANCE

Ruven Pillay and Christian Lahanier
Centre de Recherche et de Restauration des Musées de France, Paris, FRANCE

The CRISATEL multispectral acquisition system is dedicated to the digital archiving of fine art paintings. It is composed of a dynamic lighting system and of a high resolution camera equipped with a CCD linear array, 13 interference filters and several built-in electronically controlled mechanisms. A custom calibration procedure has been designed and implemented. It allows us to select the parameters to be used for the raw image acquisition and to collect experimental data, which will be used in the post processing stage to correct the obtained multispectral images. Various techniques have been tested and compared in order to reconstruct the spectral reflectance curve of the painting surface imaged in each pixel. Realistic color rendering under any illuminant can then be obtained from this spectral reconstruction. The results obtained with the CRISATEL acquisition system and the associated multispectral image processing are shown on two art painting examples.

Journal of Imaging Science and Technology 49: 563–573 (2005)

Introduction

This article presents the management of the high resolution and multispectral imaging system developed as part of the CRISATEL European Union project. This system is dedicated to the digital archiving of canvas paintings.[1] In this field the main problem is to obtain an image representation independent of any specific illuminant and be able to provide high fidelity displays or reproductions of the paintings in various controlled environments. This can be achieved by reconstructing the spectral reflectance curves at every sampled point of the digitized surface, since a representation based on object reflectance is independent of the illuminant used during the acquisition stage. This spectral reconstruction problem has been widely studied in the multispectral color community; see for instance the works of Burns and Berns[2] or König and Praefcke.[3] Some previous applications to fine art paintings and to pigment spectral reconstruction can be found in the works of Maître et al.,[4] Haneishi et al.[5] or Farrell et al.[6]

The hardware of the CRISATEL multispectral imaging system has been developed by Lumiere Technology.[7] It is composed of a dynamic electronically controlled lighting system and of a high resolution digital CCD camera equipped with 13 narrow band interference filters. A complete evaluation of the CRISATEL camera had first been done,[8] partly in collaboration with the scientific department of The National Gallery, London. This evaluation stage has provided us with the necessary knowledge for the design and the implementation of a complete calibration procedure.

When the system is calibrated, each digital acquisition of a painting delivers 13 single band images at high resolution and with a high dynamic range. We have applied and compared various spectral reconstruction methods to recover from these images the spectral reflectance of the painting surface elements that are imaged in every pixel. This representation allows us to faithfully simulate afterwards the rendering of the scanned painting under any illuminant.

This article is organized as follows. We first give a brief description of the CRISATEL acquisition system and then present the calibration procedure designed and implemented for this system. Afterwards a section compares the results of various spectral reconstruction techniques on a calibrated multispectral image of a color chart. We finally illustrate the spectral reconstruction with the color rendering of two canvas paintings and the simulation of illuminant changes.

Acquisition System Description

The CRISATEL multispectral camera is a digital camera based on a charge-coupled device (CCD) composed of a 12,000 pixel linear array. This array is vertically

Original manuscript received July 8, 2004

Corresponding Author: A. Ribes, ribes@shfj.cea.fr

Supplemental Material—Figures 9–11 can be found in color on the IS&T website (www.imaging.org) for a period of no less than two years from the date of publication.

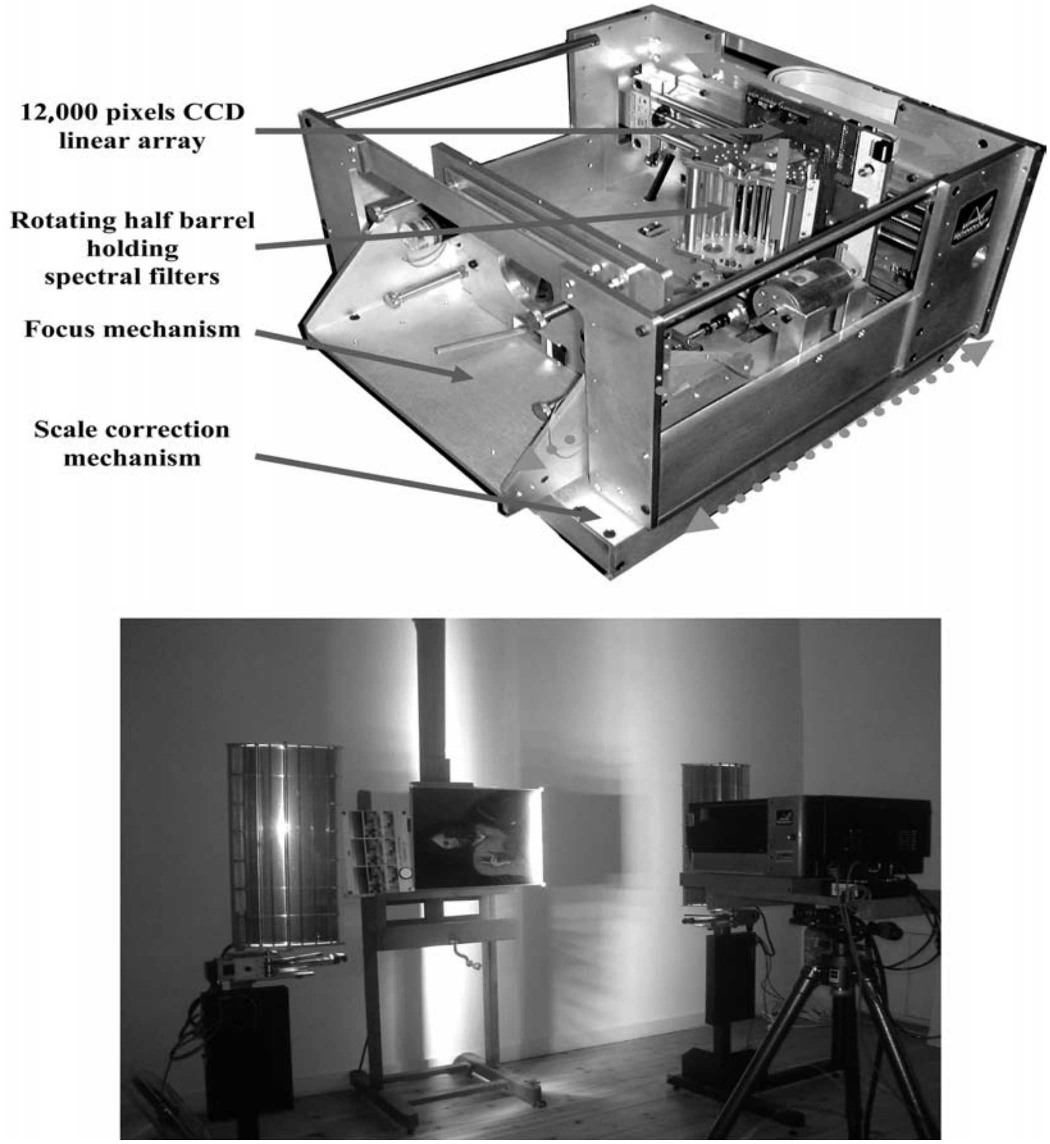

Figure 1. Top: internal camera structure and system components of the CRISATEL camera (©Lumiere Technology). Dotted arrows indicate motorized mechanisms. Bottom: classical set-up of the CRISATEL camera in front of a painting and of the two synchronized elliptical projectors on both side of the painting.

mounted and mechanically displaced along a horizontal axis by a precise step motor. The system is able to scan up to 20,000 vertical lines. This means that images up to 12,000 by 20,000 square pixels can be generated. The current camera is equipped with a built-in half-barrel mechanism that automatically positions a set of 13 interference filters, ten filters covering the visible spectrum and the other three covering the near infrared. There is an extra position without filter in the half-barrel allowing panchromatic acquisitions. The spectral transmittance curves of the filters in the visible range have 40 nm bandwidth and are equally spaced from 380 to 780 nm with 40 nm steps. In the infrared range the filter transmittances have 100 nm bandwidth and are centred at 800, 900 and 1000 nm. The filters have been manufactured by Melles Griot. An image of the internal components of the camera can be seen in Fig. 1. The 13 spectral filter transmittances are shown in Fig. 2.

Since the spectral transmittance of an interference filter is known to depend on the angle of incidence of the light, we have measured using a Monolight spectrophotometer the angular dependency of the ten filters covering the visible range (see Fig. 3). There is a 1.5 nm shift towards the low wavelengths at 5 degrees and a 4.5 nm shift at 10 degrees with nearly no distortion of the spectral curve shape. Since the maximum angle of incidence within the CRISATEL camera is around 7 degrees, the maximum wavelength shift is less than 3nm. This means that practically no spectral inhomogeneity in a channel image is introduced by the variation of the angle of incidence in the image formation.

For readout operations the CCD linear array uses two channels which process the pixels on even and odd positions respectively. In each CCD channel the raw signal passes through an analogue amplifier. Each amplifier has two control parameters, an offset and a

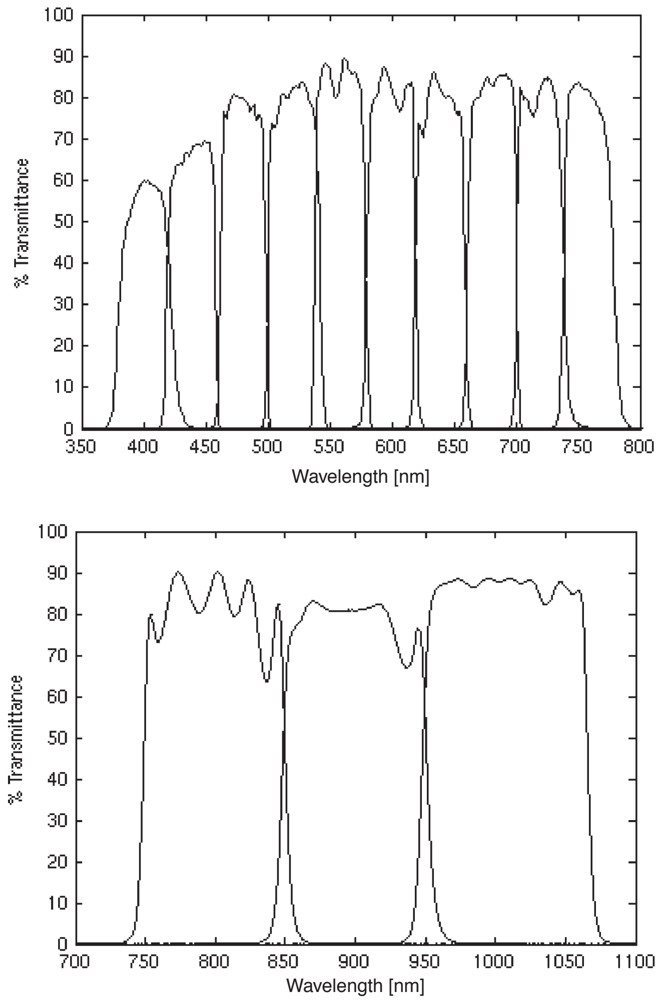

Figure 2. Top: Transmittance of the 10 visible filters measured with a Hitachi spectrophotometer. Bottom: Transmittance of the 3 infrared filters measured with a Monolight spectrophotometer.

gain. The analog signal delivered by the amplifier for each pixel is then quantized into 12 bits by an analogue to digital converter (ADC).

For a given scene and a given set-up of the lighting system, there remain two physical parameters which allow us to control the amplitude of the signal: the aperture of the optical lens and the exposure time. Both factors can modify the number of incident photons trapped in each individual CCD cell. The aperture of our dedicated optical lens is kept fixed during an acquisition with all filters and therefore does not need to be controlled electronically. The exposure time can be automatically set up and changed from 1.3 ms to 200 ms by steps of 0.1 ms.

A step motor controls the focus of the lens precisely. Due to the remaining chromatic aberration of the lens and to the different thicknesses of the filters, the focal length is not exactly the same for the 13 channels resulting in images of slightly different scale. The multispectral camera provides a displacement system of the full camera body that can partly compensate these differences in scale for every spectral channel (see Fig. 1). Despite this compensation some misalignments of several pixels can still be observed between the images acquired with different filters. A digital post-processing step has, therefore, been developed to align the full set of 13 images by using a correlation technique.

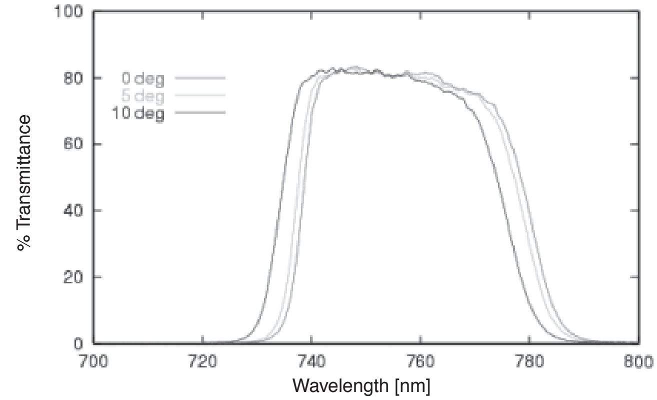

Figure 3. Angular dependency of the spectral transmittance of a filter. Measures performed by Haida Liang at the National Gallery of London.

The lighting system is composed of two elliptical projectors equipped with either Halogen lamps or HQI bulbs. Whereas the optical axis of the camera is positioned perpendicularly to the painting surface, the projectors are positioned laterally at the left and right sides of the painting (see Fig. 1, bottom). They each project a narrow vertical light beam. Both projectors rotate synchronously with the CCD displacement, their projected beam remaining superposed on the surface of the painting while they are scanning it.

System Calibration

As mentioned in the introduction, an evaluation of the CRISATEL multispectral camera has been performed.[8] The data collected during this evaluation formed the basis for the design and the implementation of a calibration procedure. Such a procedure needs to be done after any new set-up of the acquisition system. It consists in a series of experiments which allow us first to select the parameters to be used for the acquisition of images, and second to collect experimental data which will be used in a post-processing stage to correct the obtained multispectral images.

When the positions of the camera and of the two projectors have been fixed prior to a new acquisition session, we warm up the lighting system and perform on a painting the following preliminary steps before proceeding to the calibration:

- The camera aperture is manually chosen. It must satisfy a good compromise between a large depth of field over the surface we desire to scan and a sufficient intensity of the light reaching the camera image plane.
- The camera is focused with each one of its 13 filters. This is performed by built-in interactive software provided by the camera manufacturer. When in focus, the exact position of the lens controlled by a step motor is stored for each image channel.

A homogeneous diffuse white board is then positioned in the plane where paintings will be scanned. The

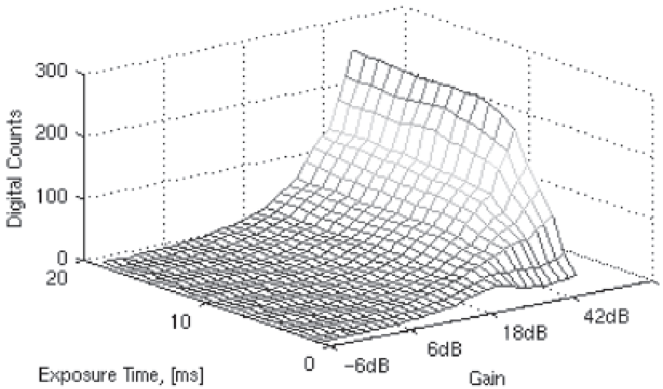

Figure 4. Standard deviation of the CCD dark current noise shown as a function of the exposure time and the amplifier gain.

calibration procedure is then composed of the following steps:

- Selection of the remaining camera parameters: gain and offset of the two CCD amplifiers, exposure time. They should be chosen such that the images present a high dynamic range with a maximal signal to noise ratio.
- Measurement of the inhomogeneity of the lighting spatial distribution on the painting plane. At the end of the procedure, corrections should be applied in order to compensate for the lighting and the corrected images are expected to have a high dynamic range and good spatial lighting homogeneity.
- Measurement of the inhomogeneity in the physical response of every pixel of the CCD linear array (dark current contribution, photosensitivity).

Fixing Camera Parameters

The first step of the calibration aims to obtain a high dynamic range by appropriately fixing the remaining camera parameters, i.e., the gain and offset of the two CCD amplifiers and the exposure time for each one of the 13 channels. During the camera evaluation a set of experiments have been conducted with all combinations of amplifier gain and exposure time to measure the noise introduced on the signal by the dark current and to determine the noise mean m and the noise standard deviation σ. Figure 4 shows the relationship between σ and the values chosen for the gain and the exposure time. The dark current standard deviation σ is evaluated in digital counts on the 12 bits output signal. We clearly observe that there is a nonlinear relationship between these parameters. The amplifier gain should remain limited as the noise increases rapidly with this parameter. As a consequence, the amplifier gain can be fixed to a value giving a compromise between low noise and an acceptable acquisition time. We choose this value to be 8 dB.

The amplifier gain having been selected, the amplifier offset can be fixed too. We should choose the offset such as to compensate for the dark current mean m in order to obtain the maximum dynamic range. However the noise standard deviation limits the offset value that can be used if we want to keep all noise variability in the image and to avoid any saturation effect with the loss of one part of the information received by the CCD. By considering that in a Gaussian distribution the dark current value of a pixel is on the interval $[m - 3\sigma, m + 3\sigma]$ with 99.73% probability, we choose an offset value which does not truncate the lower bound of this interval.

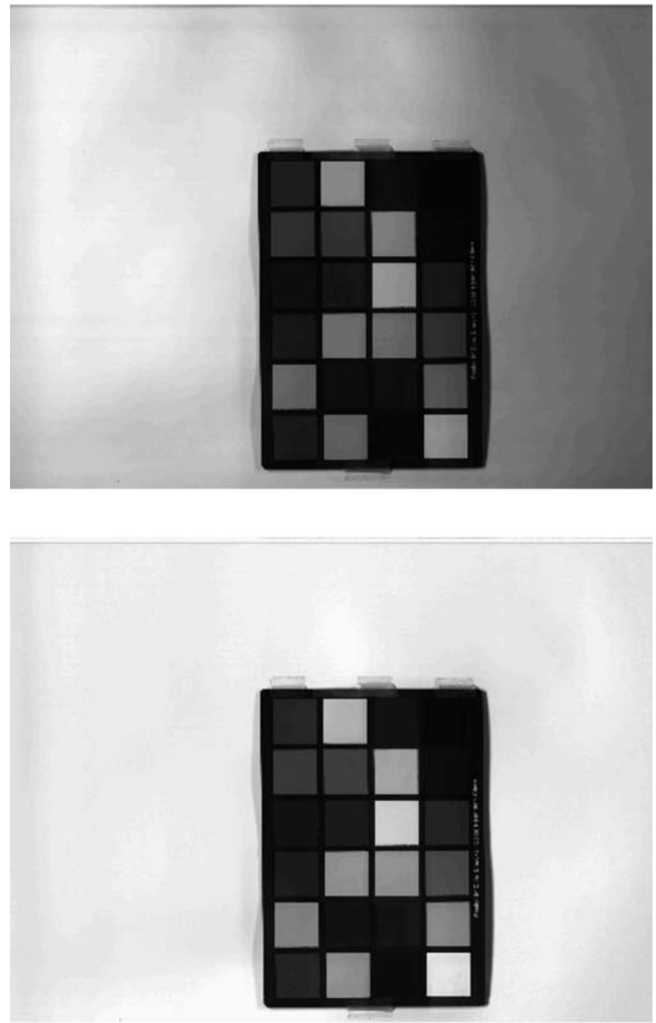

Figure 5. Top: raw image of a Macbeth chart obtained from the CRISATEL camera. Bottom: same image after illuminant inhomogeneity correction.

Once both the gain and offset of the amplifiers are fixed, the only free parameter left is the exposure time. Finding the exposure time that gives the highest dynamic range while avoiding CCD saturation simply requires solving, in principle, a one-dimensional optimization problem. Unfortunately this is very delicate in practice due to the inhomogeneity of the lighting system. An important part of the calibration is then dedicated to the robust quest for a suitable value of this parameter. The procedure is based on an optimization of the exposure time when imaging a diffuse white board positioned on the painting's image plane. This procedure involves various spatial analysis algorithms that take into account the inhomogeneity of the light distribution within the image. The details of this part can be founded in chapter 6 of Ribés' Ph.D. thesis.[9]

Spatial Distribution of the Lighting

Once the camera parameters have been fixed we capture a multispectral image of the white diffuse board. It provides us with 13 maps that characterize the spatial

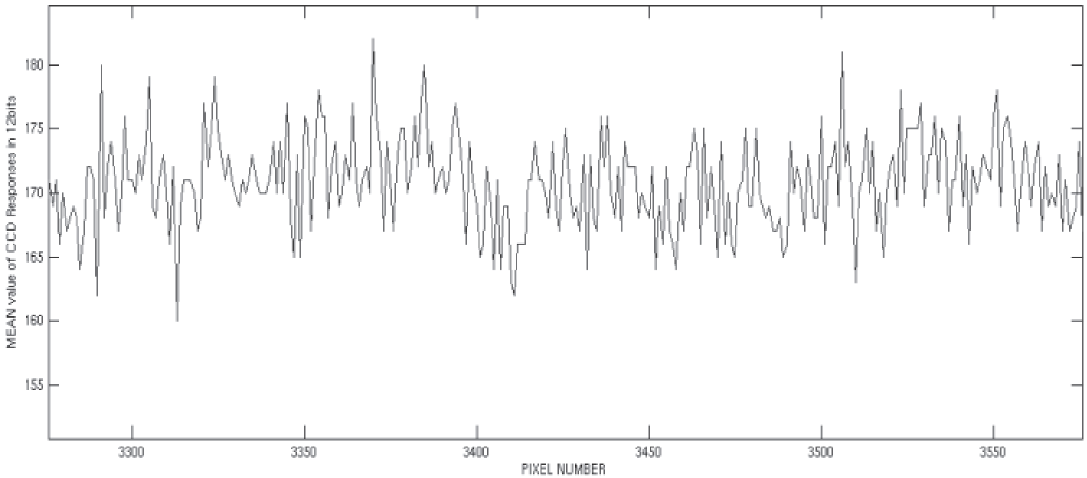

Figure 6. Mean value of the dark current on a detail of an area of the CCD linear array.

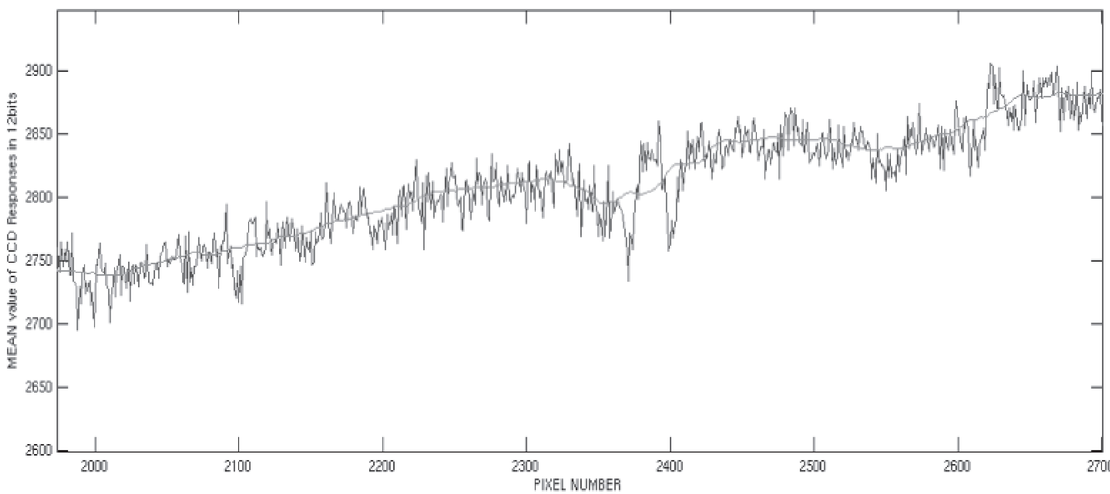

Figure 7. Mean value of the CCD pixels imaging a white board with a diffuser on a detail of an area of the CCD. Note the difference between the raw values (jagged curve) and their low-pass filtered values (smooth curve).

inhomogeneity distribution of the light sources within each channel. A map per channel of the lighting non-homogeneity is necessary because we can observe non-trivial differences between them due to the use of two lighting systems which have not strictly equal spectral lighting distribution. The 13 acquired maps will serve as the lighting correction for the painting images in each individual channel.

Per Pixel Dark Current

The last step of the calibration procedure is the measurement of the inhomogeneity in the physical response of the CCD linear array cells. The camera lens is first occluded by using an opaque (metallic) cap. In the case of the CRISATEL camera there is a built-in electronically controlled mechanism that allows the occlusion of the camera. No light then reaches the CCD and we can take a black image without switching off the lighting system. We then estimate the dark noise mean value μ_i and the standard deviation σ_i in each cell i of the CCD linear array from the distribution of the image pixel values along the horizontal line which is scanned by that cell. Figure 6 shows the dark noise mean value μ_i on a small portion of the CCD linear array cells. We clearly see that the variability of dark noise between pixels must be taken into account.

Combining these two statistics we build a table of 12,000 dark current correction values ($\mu_i - 3\sigma_i$) which will be subtracted from the pixel value p_i issued from the i-th cell, $i = 1,\ldots,12{,}000$, during the acquisition stage to obtain the resulting corrected pixel value v_i:

$$v_i = p_i - (\mu_i - 3\sigma_i). \tag{1}$$

Per Pixel Gain

The diffuse white board having been positioned, a diffuser is introduced in the optical path in order to obtain a bright and smooth light field in the camera image plan. The CRISATEL camera has a built-in electronic mechanism that allows the interposition of the diffuser in the optical path. It guaranties that the spatial distribution of the light intensity reaching the CCD cells is continuous with only low frequency components. We then acquire an image.

In Fig. 7 we show the graph of the pixel mean value on a small portion of the CCD cells. In spite of the use

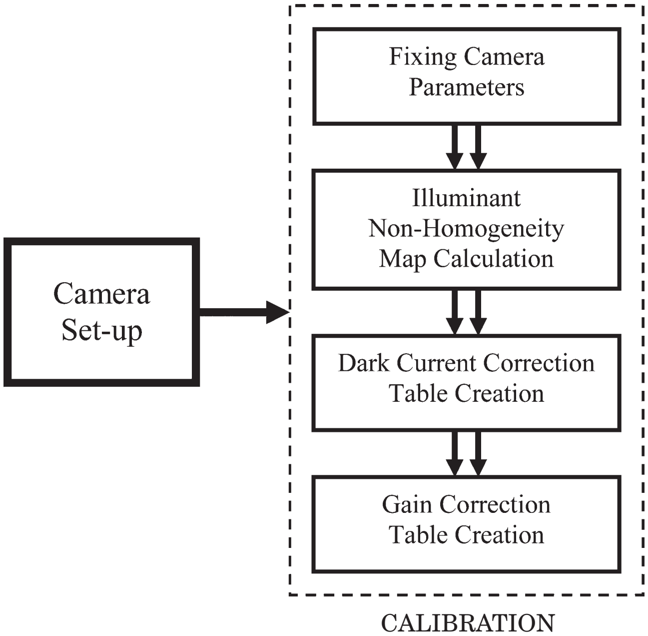

Figure 8. Flow chart summarizing the calibration procedure workflow.

of a diffuser we still observe high frequencies which are due to the non-homogeneity of cell sensitivity. We have superimposed the same data after it has been low-pass filtered. This filtered curve estimates the expected spatial energy distribution of the lighting on the CCD. This part of the calibration allows us to evaluate the gain compensation g_i, $i = 1\ldots12{,}000$, to be applied for each cell in order to correct the local differences between both curves.

Let b_i be the actual i-th pixel value, n_i the dark current noise offset per pixel and v_i the underlying ideal signal. In the case where the CCD array would present no dark noise and the CCD cells would have exactly the same sensitivity we would have $b_i = v_i$. In the real case this relationship becomes $b_i = g_i\, v_i + n_i$.

Let a_i be the value resulting from a mean on a window of W cells centred on the i-th cell. By assuming that the underlying low frequency signal v_i is locally linear on W we obtain the following relation:

$$a_i = \frac{1}{W}\sum_W g_i v_i + n_i = v_i \frac{1}{W}\sum_W g_i + \frac{1}{W}\sum_W n_i\,. \tag{2}$$

By assuming that the mean of g_i on the window W is equal to 1 we can estimate v_i as:

$$v_i = a_i - \frac{1}{W}\sum_W n_i\,. \tag{3}$$

The gain is then defined as

$$g_i = \frac{b_i - n_i}{a_i - \frac{1}{W}\sum_W n_i}\,. \tag{4}$$

Fully Automatic Calibration Procedure

The CRISATEL calibration procedure is fully automatic. This aspect is not a trivial consequence of our design but it was a prerequisite and has been studied carefully in order to minimize user interaction. During the set-up the camera and the projectors have to be first properly installed to acquire paintings, then the lens aperture selected and the focus properly adjusted for all channels. This set-up takes typically more than 30 minutes. Then, the user has to proceed to the calibration before starting the multispectral image acquisition. The user needs only to warm up the lamps and position a white board in front of the camera. Then he has only to launch the calibration procedure.

Occluding the camera lens or introducing a diffuser into the optical path are seemingly easy manual operations but, in practice, this proved tedious and time consuming. Our work with Lumiere Technology led the company to integrate into the camera the two electronically controlled mechanical displacement systems which allow occlusion and diffusion respectively. They make the calibration self-contained. A typical calibration takes about 25 minutes.

Figure 8 shows a flow chart summarizing the successive steps of the calibration procedure.

Spectral Reconstruction

In this section we compare various reconstruction techniques of the spectral reflectance curves using images acquired with the CRISATEL multispectral system. These comparisons are performed on calibrated and corrected images.

In order to illustrate the spectral reflectance reconstruction capabilities of the CRISATEL system we focus on a simple experiment done on a multispectral image of the color chart produced by the pigment company Pébéo for the CRISATEL project. This chart is a juxtaposition of three similar sets of color patches which differ only on the application of a varnish layer: the first set has no varnish, the second set has a thin layer of matte varnish and the third set has a layer of brilliant varnish. Each set contains 117 patches: 81 color patches and 36 grey patches. The 81 color patches are mostly composed of a mixture of several pigments: while some of them contain only one pigment, others contain up to four pigments. They are sorted in a square of 9 columns and 9 lines according to their hue values in the CIELAB color space. The 36 greyscale patches are composed of a mixture of two black and white pigments and are sorted in a 9 columns per 4 lines rectangle. This chart has been measured with a Minolta 2600d spectrocolorimeter consisting on a Silicon photodiode array, an integrating sphere with a d/8 geometry and a xenon flash lamp, specular reflection was excluded from the measurements. This spectrometer returns reflectance values in the wavelength range 360 to 740 nm. In addition, an ultraviolet filter was used to block light below 400 nm, in order to avoid eventual fluorescence effects.

Considering the 117 matte-varnished patches of the color chart we obtain two different kinds of data issued from the 10 channels of the multispectral image which belong to the visible range:

1. A 10 line and 117 column matrix containing in each of its elements the mean camera response in the corresponding camera channel and on the corresponding color patch.
2. A 10 line and $117 \times S$ column matrix containing in its columns the 10 non averaged pixel camera responses, S being the number of pixels analysed onto each color patch. S has been set to 200 in our experiments.

TABLE I. Comparing Spectral Errors for Different Spectral Reconstruction Techniques on the CRISATEL Color Chart

	Non averaged test set	Training Set
Smoothing Inverse	0.034203	0.030948
Hardeberg Inverse	0.024437	0.021479
Cubic Spline Interpolation	0.023805	0.020306
MDST Interpolation	0.027842	0.024060
SVD Pseudo-inverse	0.015878	0.010770
Non-averaged Learning Pseudo-inverse	0.015258	0.010225
NNLS	0.018454	0.016108
Mixture Density Network	0.012161	0.007171

TABLE II. Comparing CIELAB Color Differences for Spectral Reconstruction Techniques on the CRISATEL Color Chart

	Non averaged test set	Training Set
Smoothing Inverse	4.51	4.69
Hardeberg Inverse	4.44	4.74
Cubic Spline Interpolation	3.59	4.02
MDST Interpolation	4.86	4.79
SVD Pseudo-inverse	3.50	2.58
Non-averaged Learning Pseudo-inverse	3.33	2.45
NNLS	3.53	3.82
Mixture Density Network	2.48	1.88

Based on this data we compare different spectral reflectance reconstruction methods proposed in the literature:

- two methods based on the inversion of the physical measures of the acquisition system: the Smoothing Inverse[10] and the Hardeberg Inverse,[11]
- two interpolation methods using cubic splines and the MDST[12] method,
- four learning based methods: SVD Pseudo-inverse,[13] Non-averaged Learning Pseudo-inverse,[14] Non negative Least Square[14] (NNLS) and Mixture Density Networks.[15]

The final four methods mentioned above are based on the learning over a training set of spectral reflectances and their corresponding camera responses. We have then divided the CRISATEL chart into two sets, one used for training and the other for testing. This leads to four different data sets: averaged train, non-averaged train, averaged test and non-averaged test. In our experiments train and test sets have the same size, the above data matrices having been simply divided into two non-intersecting sets by taking even elements for one set and odd elements for the other. Other appropriate constructions of training and test sets exist but they are out of the scope of this article. The sets chosen above are sufficient to clearly illustrate the capabilities of the spectral reconstruction techniques applied to the CRISATEL multispectral images. The averaged camera responses sets can be considered as less influenced by noise than the non-averaged ones. But the non-averaged sets present a more realistic pixel-based situation.

We present in Table I the spectral reflectance reconstruction mean errors obtained by using the different reconstruction techniques. The error measure used for a given reference spectral reflectance curve $r_m(\lambda_i)$, $i = 1 \ldots N$ (curve measured with the spectroradiometer) is the Absolute Mean Error (ABE):

$$ABE = \frac{1}{n}\sum_{i=1}^{N}\left|r_m(\lambda_i) - r_e(\lambda_i)\right| \qquad (5)$$

where $r_e(\lambda_i)$, $i = 1 \ldots N$, is the spectral reflectance curve estimated by a reconstruction method, λ_i represents the sampled wavelengths, and N is the number of samples used to represent the curve. In this case $N = 34$ (number of samples between 400 and 740 nm at 10 nm intervals).

We show here the results corresponding to the non-averaged test set because it is more realistic, as it includes very noisy camera responses. Results over the training set are included for comparison.

In Table II we present the mean CIELAB94[16] errors associated to each method. The results follow a very similar behavior than those calculated for the spectral errors shown in Table I. A full analysis of the results can be found in chapter 8 of Ribés' Ph.D. thesis.[9]

Direct inversion methods require the measure of the CCD sensitivity and of the CRISATEL filter transmittances. Although these measures have been done carefully by using a monochromator and a calibrated radiometer for the CCD sensitivity and a spectrophotometer for the filter transmittances, we note that direct inversion methods such as Smoothing Inverse and Hardeberg Inverse perform badly compared to the other methods. We believe that this lack of accuracy is mainly due to the fact that our training and test sets all belong to the specific canvas-painting environment, which favors training methods.

We can also remark that methods based on interpolation (MDST and Cubic Spline) provide intermediate results, Cubic Spline being better than MDST in that case. Smaller errors are obtained with the Mixture Density Networks followed by the Non-averaged Learning Pseudo-inverse method.

Art Work Spectral Reconstruction

In this section we show two illustrative examples of spectral reflectance reconstruction on real fine art paintings: one work painted by Georges de la Tour and another by Guillaume Fouace.

A multispectral image of a painting by Georges de la Tour, "Saint-Jacques le Mineur" was acquired at Musée Toulouse Lautrec, Albi, France, on December 2003 by a team of experts of the CRISATEL project. Nine other paintings were also acquired during this session. In this acquisition the calibration procedure described in this article was used. Geometrical and radiometric post-processing corrections were then performed. In Fig. 9, (*available in color as Supplemental Material which can be found on the IS&T website (www.imaging.org) for a period of no less than two years from the date of publication*) we show an image of the acquired painting. It has been obtained by highly subsampling the original multispectral image acquired at full resolution of the CRISATEL system (20,000 × 12,000 pixels). To produce the color image the spectral reflectance curves of the selected pixels have been first reconstructed by using a Mixture Density Network with 12 neurons in its hidden layer and 7 Gaussians composing the mixture model.[8] The reconstructed spectral reflectance curves have been then projected into the sRGB color space using the daylight D65 illuminant. Note that

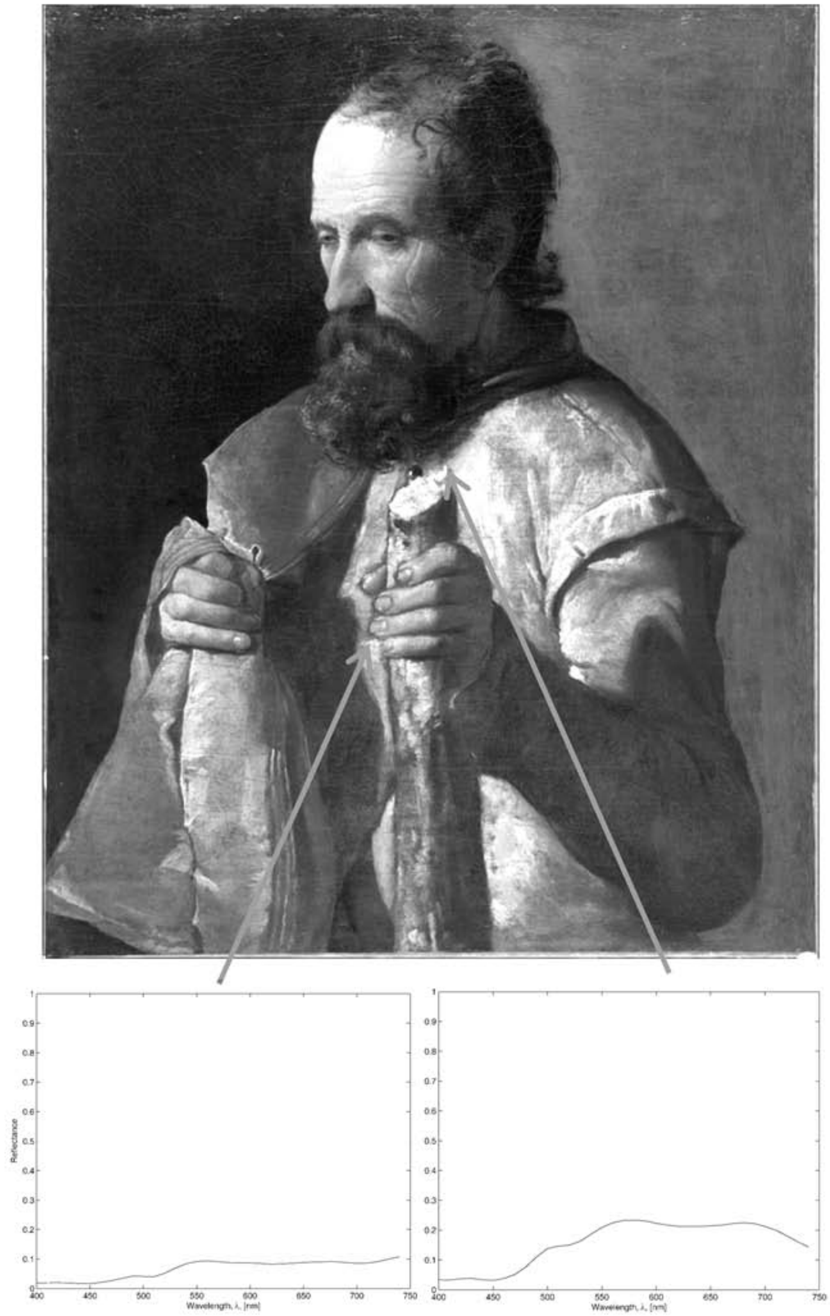

Figure 9. Top: painting Saint Jacques le Mineur by Georges de la Tour (Musée Toulouse Lautrec, Albi, France). Bottom: spectral reconstruction of the reflectance curves on two pixels of the multispectral image. The spectral reflectance curves have been estimated using a Mixture Density Network. *Supplemental Material—Figure 9 can be found in color on the IS&T website (www.imaging.org) for a period of no less than two years from the date of publication.*

the printed image on the medium you see is not calibrated. Two examples of spectral curves are shown in Fig. 9 along with their corresponding positions in the image. The reconstructed curves have a low reflectance and the painting itself is very dark which is typical of the style of Georges de la Tour.

"Le Départ pour Jersey" was painted by Guillaume Fouace around 1883. It was scanned by members of the CRISATEL project at the Musée Thomas Henry in Cherbourg, France. Its dimensions are 60×73.5 cm. As with the previous example it was scanned at $20{,}000 \times 12{,}000$ pixels. The image shown in Fig. 10, (*available in color as Supplemental Material which can be found on the IS&T website* (*www.imaging.org*) *for a period of no less than two years from the date of publication*), corresponds to the projection of the reconstructed spectra into the sRGB color space using daylight D65 illuminant.

The images of the above painting were fully processed at the C2RMF where several of the reconstruction methods used in this study have been implemented using VIPS.[17] VIPS is Open Source image processing software developed by the National Gallery in London for the efficient manipulation of very large images as those acquired on paintings.

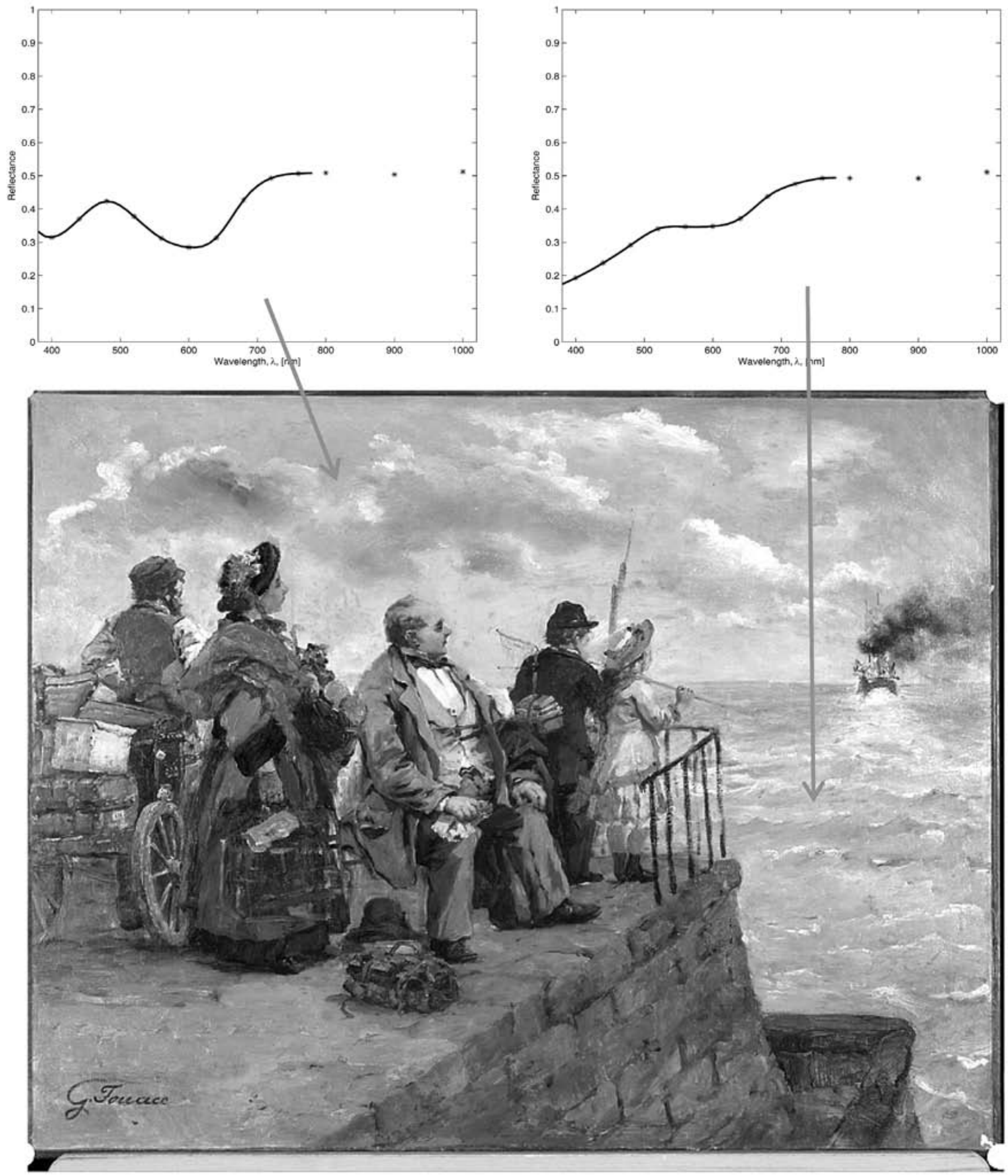

Figure 10. Bottom: color sRGB image of “Le Départ pour Jersey” painted by Guillaume Fouace (Musée Thomas Henry in Cherbourg, France). Top: reconstructed reflectance curves on two pixels of the image. The spectral reflectance curves have been interpolated from the camera responses using a cubic spline. The camera responses themselves are shown as black starts, the three infrared channels are included even they are not used for spectral reconstruction in the visible spectrum. *Supplemental Material—Figure 10 can be found in color on the IS&T website (www.imaging.org) for a period of no less than two years from the date of publication.*

Illuminant Simulation

The appearance of an object or a scene may change considerably when the illuminant changes. This is due to a combination of physical and psychophysical effects. These effects are taken into account in most color appearance models in a somewhat heuristic manner. However, such models cannot correctly predict changes for arbitrary illuminants, one important reason for this being metamerism. In fact a complete spectral description of the illuminants and of the scene is required to make a quantitative prediction of the physical phenomena involved when the illuminant is changed. Working with multispectral images and a spectral reflectance reconstruction technique provides a complete spectral description of the scene. This makes illuminant simulation a straightforward application of the CRISATEL multispectral system presented in this article. The aim of this section is not to quantify the precision of the simulation but just to illustrate and visually validate the correct behavior of the CRISATEL system.

For art paintings, a computer tool implementing illuminant simulation can be of great aid. A curator

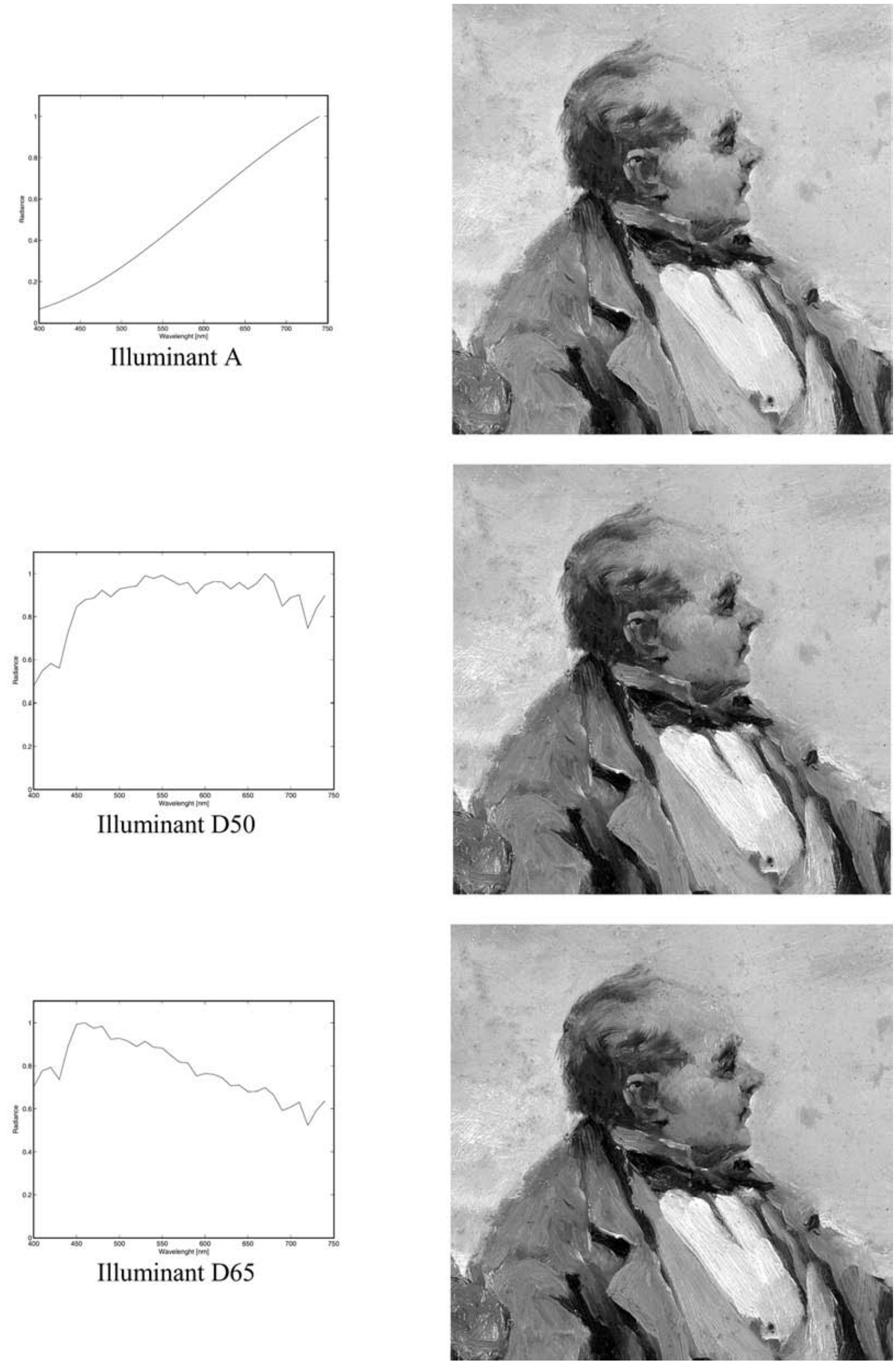

Figure 11. Illuminant simulation to produce a sRGB color image of the head of the seated man in "Le Départ pour Jersey" S*upplemental Material—Figure 11 can be found in color on the IS&T website (www.imaging.org) for a period of no less than two years from the date of publication.*

would find such a tool very useful in deciding upon appropriate light sources for an art exhibition with the original or, for instance, when having to produce a high quality printed reproduction of a painting under specific lighting conditions.

Simulating the illuminant is a straightforward process when it can be applied to each pixel of a multispectral image. It has been already applied to obtain Figs. 9 and 10. First the spectral reflectance curve $\tilde{\mathbf{r}}$ of the surface imaged in a pixel is reconstructed from its multispectral image values by using any of the existing methods. We then calculate colorimetrically the estimated XYZ tristimulus values of the surface lit by an illuminant $\mathbf{L}_{sim}$:

$$\left[\tilde{X}_{sim}, \tilde{Y}_{sim}, \tilde{Z}_{sim}\right]^t = \mathbf{A}^t \mathbf{L}_{sim} \tilde{\mathbf{r}}, \tag{6}$$

where $\tilde{X}_{sim}, \tilde{Y}_{sim}$ and $\tilde{Z}_{sim}$ are the estimated XYZ tristimulus values, $\mathbf{L}_{sim}$ is the diagonal matrix corresponding to the spectral power distribution of the simulated illuminant, $\mathbf{A} = [\bar{\mathbf{x}} \quad \bar{\mathbf{y}} \quad \bar{\mathbf{z}}]$ represents the color matching functions of the XYZ-1931 reference observer. The estimated XYZ tristimulus values are then converted in the color space used for the image reproduction sRGB[18] in our case. This is achieved by a simple linear transformation followed by a gamma-correction.

In Fig. 11, *(available in color as Supplemental Material which can be found on the IS&T website (www.imaging.org) for a period of no less than two years from the date of publication)*, we show three images of a detail of the Guillaume Fouace's painting by using three different illuminants: A (tungsten), D50 and D65 (daylight at 5000° and 6500° Kelvin, respectively).

Conclusion and Future Work

In this article we have presented how the CRISATEL digital multispectral acquisition system is used for canvas painting archiving. The calibration procedure has been described. It allows the capture of high dynamic range images without saturation and provides data for a post-processing stage where the non-homogeneities of the lighting and of the CCD linear array signal can be corrected. Once the corrections have been performed, high fidelity multispectral images are obtained. These images can then be used for the spectral reconstruction of the reflectance curves. Several methods have been tested and compared. The Density Mixture Networks method seems very promising. We have illustrated this spectral reconstruction technique with the example of two museum paintings. Finally illuminant simulation can be carried out by a straightforward application of the spectral reconstruction of a multispectral image.

The CRISATEL multispectral system is now used by the C2RMF[19] for the digital acquisition of paintings from different periods and styles on a large scale in several museums in France. The main aims are to characterise the palette of the artists and, if possible, to identify the pigments by comparison of their spectral reflectance curves with a reference of pure and mixed pigments used by artists. We verify the digital results by measuring several areas on the paint surface with a spectrocolorimeter. Analysis by X Ray micro-fluorescence is additionally used to identify the chemical composition of the pigment.

Further research on high fidelity color reproduction and pigment identification will follow this work.

Acknowledgments. This work has been funded by the European Union contract IST-1999-20163-CRISATEL. We thank our project partners for their fruitful collaboration, Pascal Cotte and all his team at Lumiere Technology, Haida Liang, John Cupitt and David Saunders at the National Gallery in London and Georges Alquié and Mohamed Benchouika at the Pierre and Marie Currie University in Paris.

References

1. C. Lahanier G. Alquié, P. Cotte, C. Christofides, C. de Deyne, R. Pillay, D. Saunders, and F. Schmitt, "CRISATEL: High definition spectral digital imaging of paintings with simulation of varnish removal". *ICOM-CC 13th Triennial Meeting*, vol 1, (ICOM, Rio De Janeiro, Brazil, 2002), pp. 295–300.
2. P. D. Burns and R. S. Berns, "Analysis Multispectral Image Capture". *Proc. IS&T/SID Fourth Color Imaging Conference*, (IS&T, Springfield, VA, 1996), pp. 19–22.
3. F. König and W. Praefcke, "A multispectral scanner". Chapter in MacDonald and Luo, (Wiley, Sussex, United Kingdom, 1999), pp. 129–144.
4. H. Maître, F. Schmitt, J. Crettez, Y. Wu, and J. Y. Hardeberg. „Spectrophotometric image analysis of fine art paintings". *Proc. IS&T/SID Fourth Color Imaging Conference*. (IS&T, Springfield, VA, 1996), pp. 50–53.
5. H. Haneishi, T. Hasegawa, N. Tsumura, and Y. Miyake, "Design of Color Filters for recording Art Works". *Proc. of IS&T 50th Annual Conference*. (IS&T, Springfield, VA, 1997), pp. 369–372.
6. J. E. Farrell, J. Cupitt, D. Saunders, and B. A. Wandell." Estimating Spectral Reflectances of Digital Images of Art". *Proc. International Symposium on Multispectral Imaging and Color Reproduction for Digital Archives*. (Chiba, Japan, 1999), pp. 58–64.
7. P. Cotte and M. Dupouy, "CRISATEL High Resolution Multispectral System". *Proc. IS&T's PICS'03*, (IS&T, Springfield, VA, 2003), pp. 161–165.
8. A. Ribés, H. Brettel, F. Schmitt, H. Liang, J. Cupitt, and D. Saunders, "Color and Spectral Imaging with the CRISATEL Acquisition System". *Proc. IS&T's PICS'03,* (IS&T, Springfield, VA, 2003), pp. 215–219.
9. A. Ribés, "Analyse multispectrale et reconstruction de la réflectance spectrale de tableaux de maître". Ph.D. dissertation, (Ecole Nationale Supérieure des Télécommunications. Paris, France, 2003).
10. W. K. Pratt and C. E. Mancill. "Spectral estimation techniques for the spectral calibration of a color image scanner". *Appl. Opt.* **15**(1), pp. 73–75 (1976).
11. J. Y. Hardeberg, "Acquisition and reproduction of color images: colorimetric and multispectral approaches", Ph.D. dissertation, (Ecole Nationale Supérieure des Télécommunications. Paris, France, 1999).
12. T. Keusen, "Multispectral color system with an encoding format compatible with the conventional tristimulus model". *J. Imaging Sci. Technol.* **40**, 510–515 (1996).
13. P. D. Burns, "Analysis of image noise in multitraitement color acquisition". Ph.D. thesis, (Center for Imaging Science, Rochester Institute of Technology, Rochester, New York, 1997).
14. F. H. Imai, L. A. Taplin and E. A. Day, "Comparison of the accuracy of various transformations from multi-band image to spectral reflectance", *Technical Report of the Rochester Institute of Technology*, (RIT, Rochester, NY, 2002).
15. A. Ribés and F. Schmitt, "A Fully Automatic method for the Reconstruction of Spectral Reflectance Curves by using Mixture Density Networks", *Pattern Recognition Lett.* **24**(11), 1691–1701 (2003).
16. CIE Publication116. *Industrial Color-Difference Evaluation*, (Commission International de l'Eclairage. Vienna, Austria, 1995).
17. J. Cupitt and K. Martinez. VIPS: an image processing system for large images. *Proc. SPIE* **1663** 19–28 (1996)
18. M. Stokes, M. Anderson, S. Chandrasekar, and R. Motta, "A Standard Default Color Space for the Internet – sRGB", (International Color Consortium, 1996) www.w3.org/Graphics/Color/sRGB.html.
19. C. Lahanier, F. Schmitt, P. Le Bœuf, and G. Aitken, „Multi-spectral Digitization and 3D Modelling of Paintings and Objects for Image Content Recognition, Image Classification and Multimedia Diffusion. An Ontology Access to the C2RMF Database and Library using the CIDOC-CRM". *International Conference of Museum Digitization, Antiquities, Painting and Calligraphy*, (National Palace Museum, Taiwan), pp. 157–201.